A Gas Hold-Up Model for Slurry Bubble Columns

Vinit P. Chilekar, Chattarbir Singh, John van der Schaaf, Ben F. M. Kuster, and Jaap C. Schouten
Laboratory of Chemical Reactor Engineering, Eindhoven University of Technology, 5600 MB Eindhoven, The Netherlands

DOI 10.1002/aic.11214
Published online June 1, 2007 in Wiley InterScience (www.interscience.wiley.com).

A phenomenological model of the gas bubble hold-up in slurry bubble columns is presented. The slurry moves upward in the core of the column and downward in the annulus, resembling the riser and downer of an air-lift loop reactor, respectively. The model virtually divides the column in a riser and a downer. The cross-sectional areas of the riser and the downer are experimentally found to be approximately equal. A macroscopic momentum balance over the riser and downer gives the liquid circulation velocity. The gas bubble hold-up is modeled for two size classes: small and large. In the homogeneous regime only small gas bubbles are present. Above the regime transition velocity the churn-turbulent regime exists, characterized by the presence of small and large gas bubbles. High speed video imaging shows that the gas flow up to the regime transition velocity generates small gas bubbles and that the gas flow in excess of the regime transition velocity generates large gas bubbles. Small gas bubbles are present in the riser and in the downer and have a constant slip velocity. The Wallis drift-flux model describes the small gas bubble hold-up in the riser and in the downer. Large gas bubbles are only present in the riser. The rise velocity of the large gas bubbles is the sum of the liquid velocity and the slip velocity according to the Davies-Taylor equation. The large gas bubble hold-up is obtained from the volume of gas flowing in large gas bubbles and the rise velocity of the large gas bubbles. For a given column diameter, column height, regime transition velocity, and physical properties of a gas–liquid system, the model predicts the total gas hold-up, the hold-up of the small and the large gas bubbles, and the average superficial liquid velocity in the riser and in the downer. Two parameters in the model are determined from experiments in a 29-cm ID bubble column: the ratio of the small gas bubble hold-up in the downer to that in the riser, and the energy dissipation at the top and bottom of the column. The model describes the gas hold-up and liquid velocity data from literature with these parameter values within an error of 6%. The model shows that there is no effect of scale on the gas hold-up for columns larger than 15 cm in diameter. © 2007 American Institute of Chemical Engineers *AIChE J,* 53: 1687–1702, 2007

Keywords: bubble column, gas hold-up, modeling, liquid velocity, hydrodynamics

Introduction

Slurry bubble column (SBC) reactors are widely employed in the chemical industry as efficient gas–liquid–solid contactors, for example for aerobic fermentation and gas–liquid Fischer-Tropsch synthesis. Major advantages of a SBC reactor are its simple construction, low operating costs, and excellent heat and mass transfer characteristics.

The design of a SBC reactor requires a thorough understanding of its hydrodynamics and mass transfer characteristics. These are influenced by the physical properties of the gas, the liquid, and the solid phases, the operating parameters (pressure, temperature), and the design parameters (column

Correspondence concerning this article should be addressed to J. van der Schaaf at j.vanderschaaf@tue.nl.

diameter, distributor, internals). The gas hold-up is the most important parameter to be estimated for SBC reactor design.[1,2] All other design parameters, such as the mass transfer coefficient and the axial dispersion coefficient, are related to the gas hold-up.

The gas hold-up in SBC reactors has been extensively studied. Over 400 papers have been published concerning the modeling of gas hold-up in (slurry) bubble columns. Review articles by Shah et al.,[3] Deckwer,[4] and Joshi et al.,[5,6] give an overview of the existing gas hold-up correlations. Wild et al.[7] discuss various advantages and disadvantages of the different gas hold-up models. Until the 1980s only average hydrodynamic characteristics of SBC reactors were reported, viz. the average gas hold-up, the overall volumetric mass transfer coefficient, and the overall gas and liquid phase dispersion.[8] Individual researchers successfully described their own gas hold-up data by empirical correlations. However, these correlations often give erroneous predictions for other gas–liquid systems or other SBC reactor dimensions. Apparently, the SBC reactor hydrodynamics are too complex to be captured by a single empirical correlation. A more fundamental model that predicts gas hold-up irrespective of the gas–liquid system or column dimensions would facilitate the design of SBC reactors significantly.

Computational Fluid Dynamics (CFD) modeling is a potentially powerful tool for studying SBC reactor hydrodynamics, e.g. mixing behavior, bubble-bubble interactions at micro and meso scales.[8–11] However, CFD simulation of especially the churn-turbulent flow regime is still problematic. Proper closure relationships and phase interaction terms are not yet established[8] and reliable predictions of SBC reactor performance using CFD calculations are expected a decade or more away.[8]

Until an adequate CFD model becomes available, a phenomenological model should be used, which describes all the phenomena in a SBC reactor that are relevant to its performance. The model should be based on the underlying physics, easy to implement in SBC reactor design, and predict the average properties of the SBC reactor with a minimum of fitting parameters. This easy-to-use model, as in this work, can be seen as a trade off between time consuming CFD calculations and empirical correlations.

In this article, the estimation of the liquid circulation velocity in the column from the momentum balance and *a priori* assumed riser-downer geometry is explained, followed by a description of the complete gas hold-up model. Subsequently, experimental data on the gas hold-up and the superficial liquid velocity is presented followed by the experimental validation of the model assumptions using a pseudo-2D SBC reactor. Finally, the two parameters of the model are obtained by fitting the model to our experimental data and then validated further with other literature data.

Description of the Gas Hold-Up Model

Riser-downer geometry

To estimate the liquid circulation velocity, a SBC reactor is virtually divided into a riser and a downer, analogous to an air-lift loop reactor, as shown in Figure 1. Rietema and Ottengraf,[12] Rice et al.,[13] and Kawase et al.[14] used a similar approach to estimate the upward and the downward liquid velocities in bubble columns. Burns and Rice[15] also assumed a similar geometry with three sections, viz., the core, the annulus, and the wall region to derive an analytical correlation for the liquid circulation velocity. This division of a SBC reactor in a riser and a downer is justified from experimentally measured radial profiles of the superficial liquid velocity, see Figure 2. Based on the velocity profile, the column is divided in two sections with an inflection point at a dimensionless radius, δ, of 0.7. The riser is the cylindrical core section in the SBC reactor with a net upward flow of the liquid. This section extends from the centre of the column until the inflection point of the superficial liquid velocity. The downer is the annular section extending from the inflection point towards the wall of the column in which the average superficial liquid velocity is directed downwards. The dimensionless radius of the riser in the homogeneous regime and in the churn-turbulent regime was experimentally found to be comparable.[15]

In the riser the superficial liquid velocity appears relatively constant for $\delta < 0.4$. The superficial liquid velocity decreases steeply from a δ value of 0.4–0.8 and is zero at the inflection point at $\delta = 0.7$. In the downer region for $\delta > 0.8$, the superficial liquid velocity profile is again relatively flat. The gas–liquid flow in the riser can be visualized as a helical plume

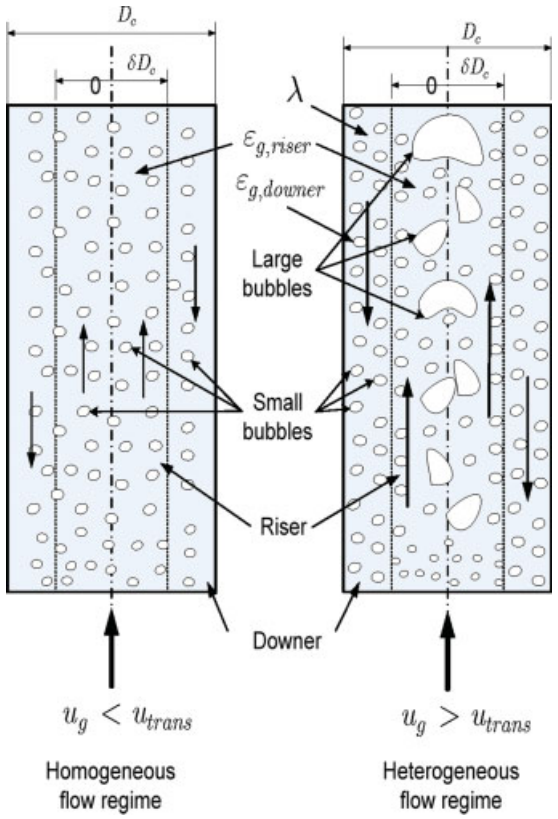

Figure 1. Representation of the riser and the downer sections in the bubble column.

[Color figure can be viewed in the online issue, which is available at www.interscience.wiley.com.]

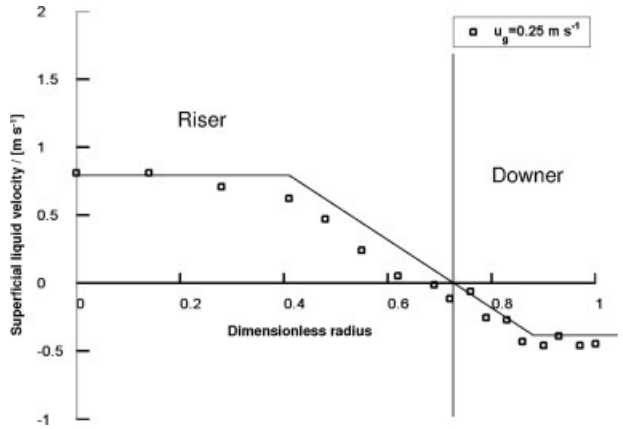

Figure 2. Radial velocity profile measured in the air-water system in the 0.29 cm inner diameter column at u_g = 0.25 m s^{-1}.

of small and large gas bubbles, meandering in the SBC reactor,[16] see Figure 3. A cross-sectional view of the liquid flow field in the SBC reactor shows that the riser is off-centered and with time it moves in a circular path as shown by the dotted lines in Figure 3b. At a given instant, a parabolic liquid velocity profile is present in the riser. However, averaging over a longer period of time, the riser covers a larger area than its cross-sectional area due to its circular movement. This is the riser-downer area depicted in Figure 3c. Thus, the parabolic liquid velocity profile in the riser becomes flat due to the periodic motion of the bubble plume. This generates a flat radial profile of the superficial liquid velocity in the riser at $\delta < 0.4$. The same holds for the downer with a negative parabolic liquid velocity. Therefore, a uniform average superficial liquid velocity is assumed in the riser and in the downer of a SBC reactor.

Based on the riser-downer geometry explained above, the SBC reactor can be visualized as an air-lift loop reactor, without a physical separation between the riser and the downer. The liquid circulation velocity can be obtained from a momentum balance over the riser and the downer as shown in the next section.

Estimation of liquid velocity using momentum balances

A momentum balance for the two phase flow along the height of the riser and the downer gives:

$$(1-\varepsilon_g)\rho_l\left(\frac{\partial}{\partial t}+u_l\frac{\partial}{\partial h}\right)u_l+\varepsilon_g\rho_g\left(\frac{\partial}{\partial t}+u_g\frac{\partial}{\partial h}\right)u_g = -L_f-\frac{\partial P}{\partial h}+((1-\varepsilon_g)\rho_l+\varepsilon_g\rho_g)g \qquad (1)$$

where u_l is the superficial liquid velocity, u_g is the superficial gas velocity, and L_f is the sum of all average volumetric momentum dissipation terms (e.g. Reynolds stress, shear stress). A steady state is assumed, with no radial or axial gradients in the riser and in the downer.[5,17] The momentum is integrated along the height, h, from point (h_1, P_1) to point (h_2, P_2), as depicted in Figure 4. Two different paths of integration are chosen, one along the riser and the other along the downer. The detailed integration and simplification of

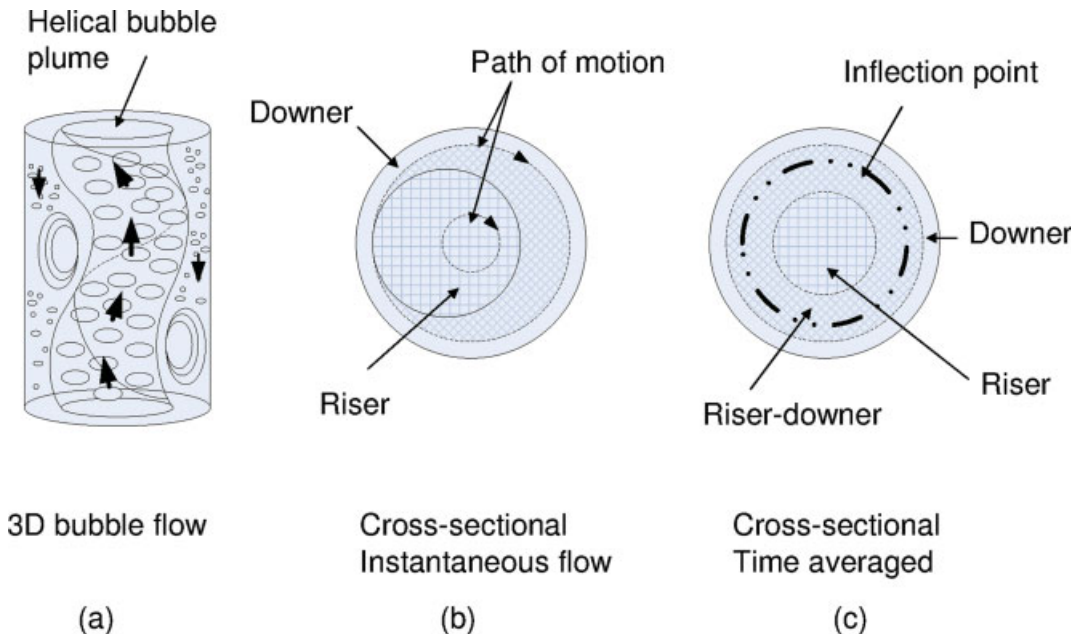

Figure 3. Graphical representation of the gas–liquid flow along the cross section of the SBC reactor.

Dynamic and time averaged motion of the helical bubble plume (riser) is depicted. [Color figure can be viewed in the online issue, which is available at www.interscience.wiley.com.]

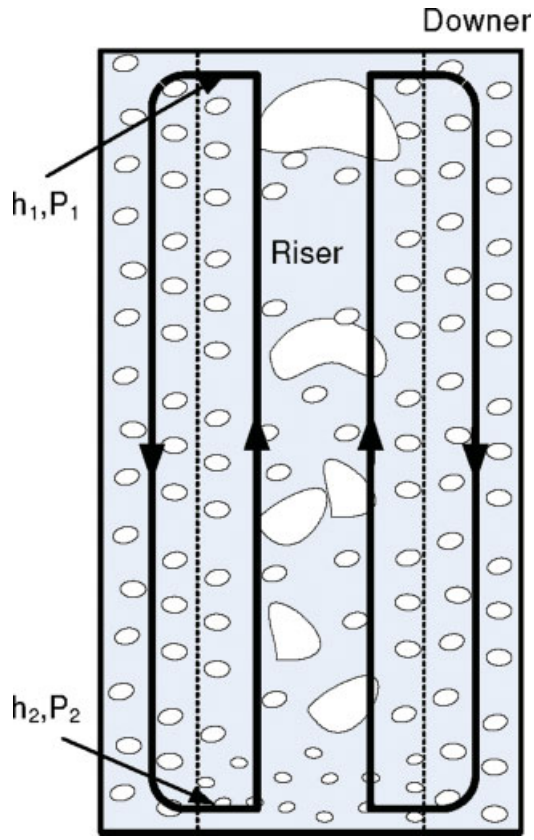

Figure 4. Representation of the application of the momentum balance at the two reference points in the geometry of the column.

(h_1, P_1) and (h_2, P_2) are the two reference points for the integration of the momentum balance. [Color figure can be viewed in the online issue, which is available at www.interscience.wiley.com.]

equations is explained in the appendix, yielding the following:

$$(\varepsilon_{g,riser} - \varepsilon_{g,downer})g = \left(\frac{f_{downer}}{R_{H,downer}} + \frac{2k}{H_s}\right)\left(\frac{\frac{1}{2}u_{l,downer}^2}{1-\varepsilon_{g,downer}}\right) + \left(\frac{f_{riser}}{R_{H,riser}}\right)\left(\frac{\frac{1}{2}u_{l,riser}^2}{1-\varepsilon_{g,riser}}\right) \quad (2)$$

where $\varepsilon_{g,riser}$ is the gas hold-up in the riser, $\varepsilon_{g,downer}$ the gas hold-up in the downer, $u_{l,riser}$ the average superficial liquid velocity in the riser, $u_{l,downer}$ the average superficial liquid velocity in the downer, H_s the height of gas liquid suspension in the column given by:

$$H_s = \frac{H}{1-\varepsilon_g} \quad (3)$$

with H the initial un-gassed liquid height in the column. The left hand side of Eq. 2 gives the driving force for liquid circulation and the right hand side gives the frictional losses in the column. The superficial liquid velocity in the riser and in the downer section is obtained from Eq. 2 provided that the gas hold-ups in the riser and in the downer are known.

The frictional losses in Eq. 2 include wall frictional losses and the frictional losses by the U-turn at the top and the bottom of the column. $R_{H,riser}$ is the hydraulic radius of the riser, and $R_{H,downer}$ is the hydraulic radius of the downer. The coefficients of friction in the riser, f_{riser}, and the downer, f_{downer}, are given by:[18]

$$f = \begin{cases} 16/Re_l & Re_l < 2100 \\ 0.079\ Re_l^{-0.25} & 10^5 > Re_l > 2100 \end{cases} \quad (4)$$

with $\mathrm{Re}_l = 2R_{H\rho l}(1-\varepsilon_g)u_l/\mu_l$. The coefficients of friction given by Eq. 4 are valid for fluid flow in a smooth pipe and are used in the model to approximate the fluid flow in the riser and in the downer.

As shown in Figure 1, the dimensionless radius of the riser is δ. The hydraulic radii of the riser and of the downer are given as:

$$R_{H,riser} = \delta D_c/4 \quad (5)$$

$$R_{H,downer} = (1-\delta)D_c/4 \quad (6)$$

The superficial liquid velocity in the downer can be calculated from a liquid mass balance as:

$$u_{l,riser}A_{riser} = u_{l,downer}A_{downer} \quad (7)$$

where A_{riser} is the cross sectional area of the riser, and A_{downer} is the cross sectional area of the downer. The gas hold-up model uses the liquid circulation velocities, $u_{l,riser}$ and $u_{l,downer}$, from Eq. 2 to calculate the gas hold-up of the large and small gas bubbles as explained in the next section.

Gas hold-up model

In this section, the basis of distinguishing between small and large gas bubbles is explained. Next, the regime transition point, which indicates the gas velocity where the transition from the homogeneous to the churn-turbulent flow regime occurs, will be discussed. Finally, a list of all the assumptions of the model is given, followed by the model equations.

Classification of gas bubbles

Krishna et al.[2,19,20] used a two-bubble-class model to describe the gas hold-up in bubble columns. The two-bubble-class model was first proposed by May[21] and Van Deemter[22] for gas–solid fluidized beds. According to Krishna et al.,[20] the gas hold-up in bubble columns can be separately characterized by two phases, viz. the dilute phase and the dense phase. The dilute phase consists of only large gas bubbles having bubble diameters greater than 6 mm. The dense phase consists of the small gas bubbles with diameters in the range of 2–6 mm, the liquid phase, and the solid (catalyst support) particles. Wesselingh[23] divides the bubbles into three classes,

based on their rise velocity:

$$u_{b,\infty} = \begin{cases} 0.23 d_b \left(\frac{g^2 \Delta\rho^2}{\rho_l \mu_l}\right)^{\frac{1}{3}}, & d_b < 1.6 \text{ mm} \\ 3\left(\frac{\sigma_l^3 g^5 \Delta\rho^5 \mu_l^2}{\rho_l^{10}}\right)^{\frac{1}{18}}, & 1.6 \text{ mm} \le d_b < 6 \text{ mm} \\ 0.71\left(\frac{g \Delta\rho d_b}{\rho_l}\right)^{\frac{1}{2}}, & d_b \ge 6 \text{ mm} \end{cases} \quad (8)$$

For an air-water system, the first class represents very small gas bubbles with diameters below 1.6 mm. Generally, these bubbles are present in negligible amounts and are not considered in the present gas hold-up modeling. The second class represents gas bubbles with a diameter in the range of 1.6–6 mm. These small gas bubbles are present in the homogeneous regime and in the churn-turbulent regime. The rise velocity of these bubbles is approximately independent of the bubble diameter. The third class represents bubbles larger than 6 mm. The large gas bubbles are only present in the churn-turbulent regime. The rise velocity of these bubbles increases with the square root of the bubble diameter, as derived by Davies and Taylor.[24]

Regime transition point

The regime transition point is the superficial gas velocity above which the flow regime changes from the homogeneous regime to the churn-turbulent regime. The criteria to identify the flow regime transition are still not clearly defined in the literature.[5,20,25] Regime transition has been described either as a transition region (range of superficial gas velocities) with two transition points[26,27] or as a single point (single superficial gas velocity) separating the homogeneous and the churn-turbulent regimes. Recently, Ruthiya et al.[28] have compared various methods to identify the regime transition point and have concluded on a physical basis that a single regime transition point describes the SBC reactor hydrodynamics, which is confirmed by the model presented here. In this work, only a single transition point is considered and the criteria that have been set to identify the regime transition point using the coherent standard deviation of measured pressure-time series[28] are used. This measured regime transition point is used as an input for the model. Existing empirical literature correlations for regime transition velocity should be regarded with caution as they are based on ambiguous definitions and detection methods of regime transitions.

Model assumptions

(i) The net flow of liquid is vertically upwards in the riser and vertically downwards in the downer.
(ii) The slip velocity between the liquid and the small gas bubbles in the riser is constant.
(iii) The regime transition point as defined by Ruthiya et al.[28] is used.
(iv) The excess gas introduced in the column at gas velocities larger than the regime transition velocity forms large gas bubbles.
(v) A fraction of the small gas bubbles is dragged into the downer by the liquid at the top of the riser and the rest of the bubbles escape out of the column. This fraction is characterized by the ratio of the small gas bubble hold-up in the downer to the small gas bubble hold-up in the riser, λ.
(vi) The size of the gas bubbles in the homogeneous flow regime ranges from 2 to 6 mm and these bubbles rise with a constant, diameter-independent, slip velocity, given by Eq. 8.
(vii) The rise velocity of the large gas bubbles is the sum of the terminal rise velocity of the large gas bubbles and the average upward superficial liquid velocity in the riser.

Model equations

The small gas bubble hold-up in the liquid phase in the riser, $\varepsilon_{g,small}$, is obtained from the constant slip velocity between the small gas bubbles and the liquid,[29] and from the Wallis drift-flux model,[30] as the difference between the interstitial velocity of the gas phase and liquid phase as:

$$U_{slip} = u_{b,\infty}^{small}(1 - \varepsilon_{g,small})^a = \frac{u_{g,riser}}{\varepsilon_{g,small}} - \frac{u_{l,riser}}{1 - \varepsilon_{g,small}} \quad (9)$$

where U_{slip} is the slip velocity, $u_{b,\infty}^{small}$ is the terminal rise velocity of the small gas bubbles obtained using Eq. 8, $\varepsilon_{g,small}$ is the small gas bubble hold-up in the liquid phase in the riser, $u_{g,riser}$ is the superficial gas velocity in the riser, $u_{l,riser}$is the superficial liquid velocity in the riser, and a is an empirical constant evaluated from the Reynolds number for the terminal rise velocity of the bubble. The power a in Eq. 9 is calculated from the Reynolds number of the rising bubble:

$$Re_\infty = \frac{u_{b,\infty}^{small} \cdot \rho_l \cdot d_{b,small}}{\mu_l} \quad (10)$$

and is obtained as:[29]

$$\begin{array}{rcl} Re_\infty < 0.2 & \Rightarrow & a = 3.65 \\ 0.2 < Re_\infty < 1.0 & \Rightarrow & a = 4.35 Re_\infty^{-0.03} - 1 \\ 1.0 < Re_\infty < 500 & \Rightarrow & a = 4.45 Re_\infty^{-0.1} - 1 \\ Re_\infty > 500 & \Rightarrow & a = 1.39 \end{array} \quad (11)$$

Equation 9 gives the small gas bubble hold-up in the liquid phase in the riser if the superficial gas velocity in the riser and the average superficial liquid velocity in the riser are known. The superficial gas velocity in the riser, $u_{g,riser}$, in Eq. 9, is given by:

$$u_{g,riser} = u_g \frac{A_{column}}{A_{riser}} + u_{g,downer} \frac{A_{downer}}{A_{riser}} \quad (12)$$

where u_g is the superficial gas velocity in the column, $u_{g,downer}$ is the superficial gas velocity in the downer, and A_{column} is the cross-sectional area of the column. In Eq. 12, the value of u_g depends upon the flow regime and is given as:

$$u_g = \begin{cases} u_g & \text{for} \quad u_g \le u_{trans} \\ u_{trans} & \text{for} \quad u_g > u_{trans} \end{cases} \quad (13)$$

$u_{g,downer}$ is obtained similar to Eq. 9 from the Wallis drift flux model[30] as:

$$u_{g,downer} = \left(u_{b,\infty}^{small}(1 - \varepsilon_{g,downer})^a + \frac{u_{l,downer}}{1 - \varepsilon_{g,downer}}\right)\varepsilon_{g,downer} \times \frac{A_{downer}}{A_{riser}} \quad (14)$$

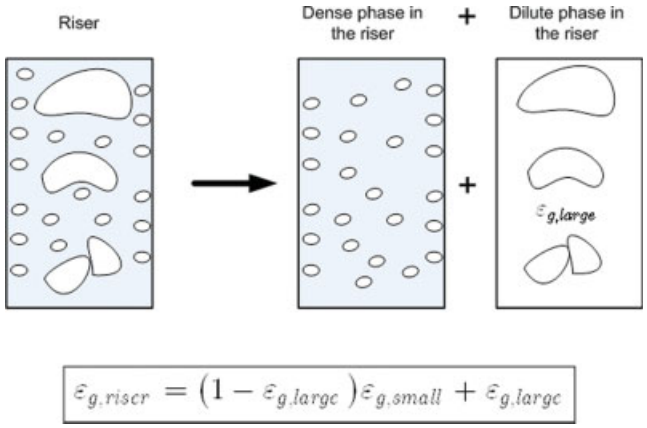

Figure 5. Schematic representation of the two-bubble-class model.

The model is applied to the riser in the churn-turbulent flow regime. $\varepsilon_{g,small}$ is the small gas bubble hold-up in the riser, and $\varepsilon_{g,riser}$ is the total gas hold-up in the riser. [Color figure can be viewed in the online issue, which is available at www.interscience.wiley.com.]

The small gas bubble hold-up in the downer is assumed to be a fraction of the small gas bubble hold-up in the riser section, see assumption (ii). It is assumed that a particular fraction of the small gas bubbles is dragged downwards by the liquid in the downer and added back to the riser near the sparger. The rest of the small gas bubbles escape out of the column. The gas hold-up of the small gas bubbles in the downer is then given as:

$$\varepsilon_{g,downer} = \lambda \varepsilon_{g,small} \tag{15}$$

where λ is the ratio of the small gas bubble hold-up in the downer to that in the riser.The riser in the column is split into two phases; a dense phase and a dilute phase (Figure 5) based on the two-bubble-class model described earlier. The large bubbles are only present in the riser section and their hold-up is given by $\varepsilon_{g,large}$. The dense phase contains only the small gas bubbles, the solid (catalyst) particles, and the liquid phase. $\varepsilon_{g,small}$ gives the hold-up of these small gas bubbles and is calculated from Eq. 9. The gas hold-up in the riser (Figure 5), according to the two-bubble-class model, is given as:

$$\varepsilon_{g,riser} = \varepsilon_{g,large} + (1 - \varepsilon_{g,large})\varepsilon_{g,small} \tag{16}$$

Since $\varepsilon_{g,small}$ represents the small gas bubble hold-up in the dense phase (liquid phase), it is converted to the effective small gas bubble hold-up in the riser, corrected with the dilute phase hold-up. Using assumption (vii), the large gas bubble hold-up in the riser is obtained as:

$$\varepsilon_{g,large} = \begin{cases} 0 & \text{for} \quad u_g \le u_{trans} \\ \frac{A_{column}}{A_{riser}} \left(\frac{u_g - u_{trans}}{u_{b,\infty}^{large} + u_{l,riser}} \right) & \text{for} \quad u_g > u_{trans} \end{cases} \tag{17}$$

where $u_{b,\infty}^{large}$ is the terminal rise velocity of the large gas bubbles given by Eq. 8. In this Equation, $d_{b,large}$ is used as the diameter of the large gas bubbles in the riser:[20]

$$d_{b,large} = d_{b,small} + 0.067(u_g - u_{trans})^{0.367} \tag{18}$$

In the above equation, $d_{b,small}$ has been added to ensure that just after the transition point the large gas bubble diameter is higher than the small gas bubble diameter. This equation has been experimentally verified by Chilekar et al.[31] It is important to note here that this equation was determined for an air-water system and is mainly valid for systems with viscosities close to that of water.

The overall gas hold-up, ε_g, is then obtained from Eqs. 15 and 16 as:

$$\varepsilon_g = \varepsilon_{g,riser} \frac{A_{riser}}{A_{column}} + \varepsilon_{g,downer} \frac{A_{downer}}{A_{column}} \tag{19}$$

Model solution

Equations 2 and 9 have to be solved simultaneously. The input parameters required for the model are: the superficial gas velocity u_g, the column diameter D_c, the initial liquid height H, the average small gas bubble diameter ($d_{b,small}$), the transition superficial gas velocity (u_{trans}), and the density and viscosity of the slurry (ρ_l, μ_l). Figure 6 gives a systematic overview of the model. All hydrodynamic properties can be calculated from the closure equations as shown in Figure 6. There are two unknown parameters in the model, viz., the ratio of the hold-ups of the small gas bubbles in the riser to the downer, λ, and the energy dissipation at the top and bottom of the column, k. These two unknown parameters are evaluated by fitting the model to experimental data.

Experiments

SBC in this study

The three-dimensional SBC reactor used in this study is schematically shown in Figure 7. The 29 cm inner diameter column was used for experiments with air-demineralised water and air-Isopar M systems. Isopar M (ExxonMobil) is a mixture of aliphatic hydrocarbons (C_6 to C_{12} mixture) used as an organic liquid in this study. The initial liquid height used for experiments was always 1.6 m above the sparger unless mentioned otherwise. Carbon and silica catalyst particles (Table 1) were present in the liquid phase in slurry concentrations ranging from 0–3 vol %. A perforated plate sparger was used with 0.5 mm diameter holes arranged in a square pitch of 7 mm. The sparger is 270 mm in diameter and 5 mm thick and has 1550 holes. The gas flow was controlled by a set of mass flow controllers (MFCs).

Pressure measurements

Fast dynamic Kulite pressure transducers (XCL-100 1.7BarA) and a Druck differential pressure transducer (type LPM 9381) were used to record the pressure time series. The combined nonlinearity, hysteresis, and repeatability of the Kulite sensor is 0.025% of its full scale output (1.7 bar) and of the Druck sensor is 0.1% of its full scale output (1 kPa), respectively. The combined error in the pressure measurements by the Kulite pressure transducers is thus less than 80 Pa and by the Druck sensors is less than 1 Pa. Pressure time series were recorded for 10–15 min at 100 Hz. In the column, the five Kulite pressure transducers were mounted flush

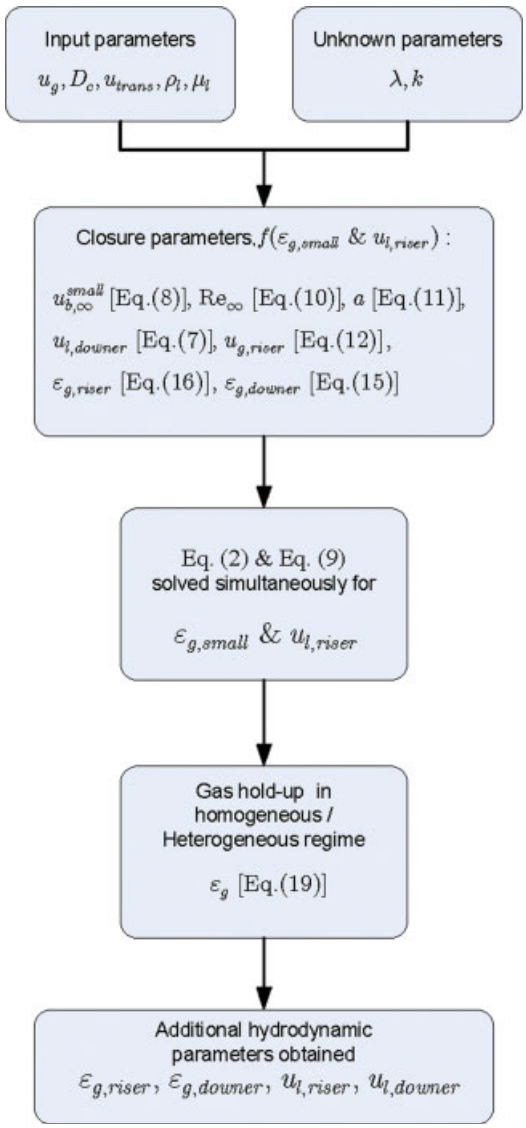

Figure 6. Overview of the gas hold-up model in which the sequential calculation of the parameters is given, starting from the input parameters needed by the model to the final output variables obtained from the model.

[Color figure can be viewed in the online issue, which is available at www.interscience.wiley.com.]

to the inner surface of the column at heights of 2, 67.5, 94, 134, and 144 cm. The flow regime transition gas velocity, u_{trans}, was obtained by performing spectral analysis of measured pressure time series as explained by Ruthiya et al.[28]

The overall gas hold-up was measured between the heights 94 and 144 cm by the Kulite pressure transducers. The overall gas hold-up was calculated from the change in the average differential pressure between the two measurement heights (i and j) as:

$$\varepsilon_{\mathrm{g}} = \frac{(\mathrm{p}_j - \mathrm{p}_i)_0 - (\mathrm{p}_j - \mathrm{p}_i)_{\mathrm{areated}}}{(\mathrm{p}_j - \mathrm{p}_i)}, \; j > i \qquad (20)$$

where i = 94 cm and j = 144 cm for the column.

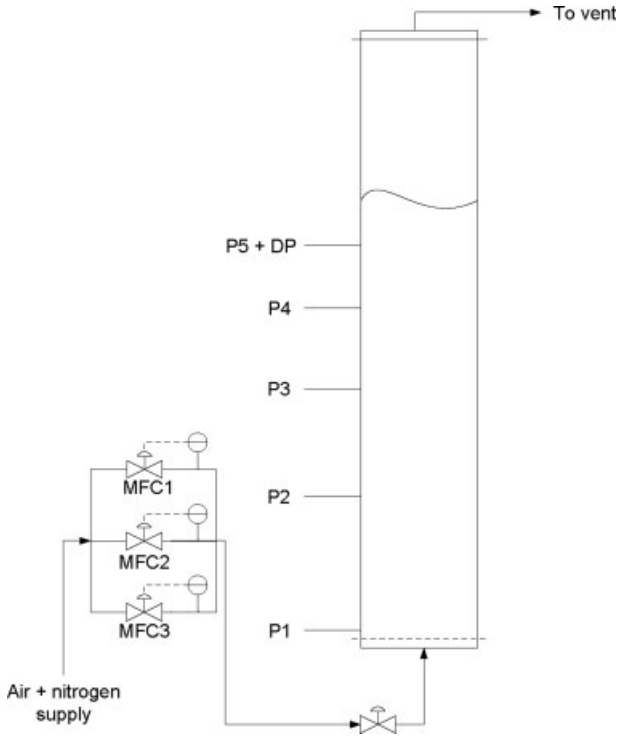

Figure 7. Typical experimental setup for a slurry bubble column as used in this study.

The sparger used was a perforated plate with 0.5 mm hole and 7 mm square pitch. The column diameter used was 29 cm. The P1–P5 are the positions of the Kulite pressure sensors and DP is the differential pressure sensor used to measure the liquid velocity.

Superficial liquid velocity

The centerline upward liquid velocity was measured using a Pitot tube. The Pitot tube was placed in the center of the column at the height of 150 cm above the sparger. The tip of the tube was directed downwards to measure the upward interstitial liquid velocity (V_1) and the tip of the tube was directed upwards to measure the downward interstitial liquid velocity (V_2). The pressure difference in the Pitot tube was measured for two minutes using a differential pressure sensor (Druck pressure sensor, type LPM 9381). The interstitial liq-

Table 1. Physical Properties of the Liquids and Catalyst Support Particles

Liquid	Dematerialized Water	Isopar M
M_{B}, kg kmol^{-1}	18	192
ρ_{L} (298 K), kg m^{-3}	998	783
μ_{L} (298 K), mPa s	1.1	2.7
σ_{L}(298 K), N m^{-1}	0.072	0.027
Solid particles	**Carbon**	**Silica**
Code	43242	G-5268
ρ_{s}, kg m^{-3}	1300	2130
d_{p}, μm	30	44
S_{BET}, m^2 g^{-1}	850	485
Pore width, nm	9.2	8.6
$V_{\mathrm{s,p}}$, ml g^{-1}	1.60	1.63
ε_{p}, dimensionless	0.65	0.85
$\Delta H_{\mathrm{aqueous}}$, mJ m^{-2}	−54	−201

uid velocities were calculated from the pressure differences ΔP_1 and ΔP_2, respectively as:

$$V_1 = \sqrt{\frac{2|\Delta P_1|}{\rho_l(1-\varepsilon_g)}}$$
$$V_2 = \sqrt{\frac{2|\Delta P_2|}{\rho_l(1-\varepsilon_g)}} \quad (21)$$

In Eq. 21, the local gas hold-up should be used, not the overall gas hold-up calculated from the pressure drop. The radial hold-up profile gives a higher local gas hold-up at the centre of the column than the measured average gas hold-up The radial hold-up profile of Ueyami and Miyauchi[32] was used with $m = 2$, to estimate the local gas hold-up and to estimate the interstitial liquid velocity correctly:

$$\varepsilon_g(r) = \varepsilon_g\left(\frac{m+2}{2}\right)(1-r^m) \quad (22)$$

This correction increases the interstitial liquid velocities slightly. With this correction, the net upflow equals the net downflow. A similar radial hold-up profile was used by Urseanu[33] to estimate the interstitial liquid velocities with a Pavlov tube. The interstitial liquid velocity was calculated as:

$$V_l = V_1 - V_2 \quad (23)$$

The superficial liquid velocity was calculated from the interstitial velocity and the corrected gas hold-up at the centre of the column.

$$u_{l,c} = V_l(1-\varepsilon_g) \quad (24)$$

The experiments show that the superficial liquid velocity profile was rather flat in the riser and downer, without much radial variation, see Figure 2. Thus, the average superficial liquid velocity is assumed to be similar to the centerline superficial liquid velocity:

$$u_{l,riser} = u_{l,c} \quad (25)$$

Video imaging

A pseudo-2D SBC reactor was used for video imaging to validate some of the assumptions of the gas hold-up model. Details of the pseudo-2D SBC reactor and video imaging and processing are explained in Ruthiya et al.[28] The video processing explained in Ruthiya et al. was used to obtain average sizes of the large gas bubbles ($d_b > 15$ mm). The huge overlapping of small gas bubbles ($d_b < 15$ mm) and clouds of small gas bubbles made the automatic video processing difficult. Therefore, the small gas bubbles, $d_b < 6$ mm, were processed manually. Ten frames from each video at a given superficial gas velocity were used to determine the bubble size distribution.

Experimental Results

Gas hold-up and superficial liquid velocity

The gas hold-up profiles for the air-water system and for the air-Isopar M system are given in Figure 8. The centerline liquid velocity was measured by the Pitot tube as explained in the previous section. The superficial liquid velocity, u_l, was calculated using Eqs. 21–25 as shown in Figure 8. In the homogeneous regime, the gas hold-up increases linearly with the superficial gas velocity and the superficial liquid velocity is relatively small until the transition gas velocity is reached. The flow regime transition velocity was measured using the pressure fluctuations technique; i.e., for air-water system $u_{trans} = 0.006$ m s^{-1} and for air-Isopar M system $u_{trans} = 0.055$ m s^{-1}. These regime transition velocities were used in fitting the model to the experimental data as explained in the next section of "Model results". Beyond the transition gas velocity increasing the gas velocity, the superficial liquid velocity increases exponentially. The gas hold-up decreases slightly and again increases at higher superficial gas velocities. In case of carbon slurries, the slight decrease in the gas hold-up is due to a decrease in the flow regime transition velocity.

Inflection point

The inflection point for the air-water system and the air-Isopar M system was experimentally verified as shown in Figure 9a, b, respectively. The inflection point for the gas–liquid systems in both flow regimes occurs at the dimensionless radius of 0.7. Similar values of the dimensionless radius are reported in the literature for the inflection point.[14,15] The volumetric liquid flow in the riser and in the downer was calculated and was found to be equal, thus verifying the correctness of the superficial liquid velocity measurements. The presence of the inflection point confirms the validity of assumption (i), which states that the net flow of liquid is vertically upward in the riser and vertically downwards in the downer.

Validating model assumptions using video imaging

The assumptions (i) and (ii) were confirmed by visual observations of the video images of the pseudo 2D SBC reactor. The video images showed that in the homogeneous flow regime, the small gas bubbles rise with a constant rise velocity in the riser. The liquid flow is upwards in the riser and downwards in the downer.

In Figure 10, the bubble size distribution of the small gas bubbles is shown at two superficial gas velocities. In Figure 10a, at $u_g = 0.001$ m s^{-1}, only small gas bubbles are present with a narrow bubble size distribution from 2 to 7 mm. This supports assumption (vi). In Figure 10b, at $u_g = 0.44$ m s^{-1}, a distinct separation in the bubble population is observed between small gas bubbles ($d_b < 6$ mm) and large gas bubbles ($d_b > 6$ mm). This coincides with the boundary for the definition of the two bubble classes: small and large gas bubbles, although this definition is not required by the model. The small gas bubbles show a normal distribution from 2 to 6 mm. These observations further support assumption (vi).

Assumption (iii) can be verified by calculating the gas flow into the large gas bubbles from the video image processing and the gas flow in the small gas bubbles from the difference between the total gas flow and the large bubble gas flow. In Figure 11, the results from the image analysis for the complete column height are shown. Up to the transition point for the pseudo-2D SBC reactor ($u_{trans} = 0.04$

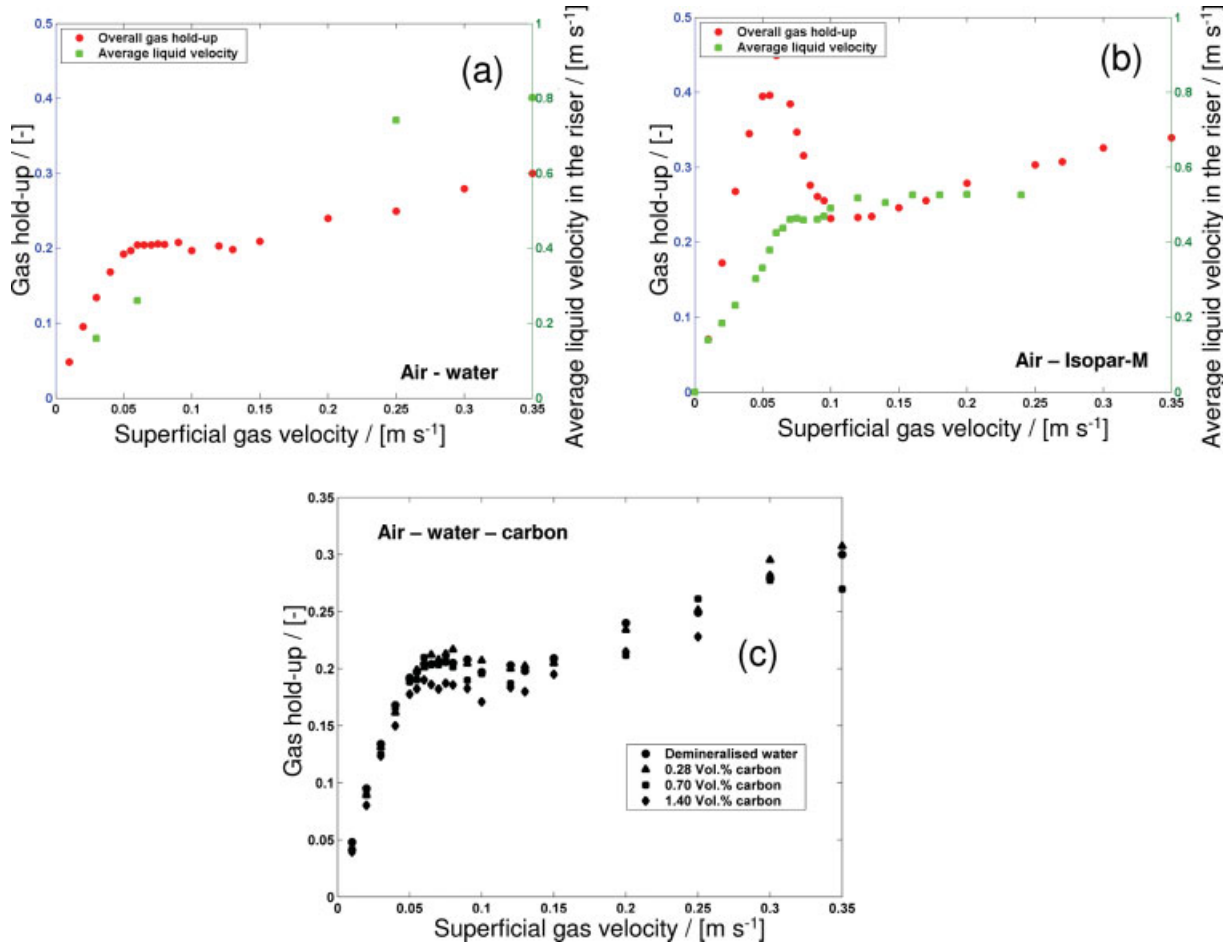

Figure 8. Overall gas hold-up and average superficial liquid velocities measured in the column.

(a) Air-demineralized water system. (b) air-Isopar M system. (c) Carbon slurries. The slurry concentrations are ranging from 0-2.8 vol %. [Color figure can be viewed in the online issue, which is available at www.interscience.wiley.com.]

m s^{-1}), all the gas introduced in the SBC reactor at the distributor generates small gas bubbles and the gas flow by the large gas bubbles is zero. Beyond the transition velocity ($u_g > 0.04$ m s^{-1}), the gas flow in the small gas bubbles is constant and all the additional gas generates large gas bubbles until $u_g = 0.25$ m s^{-1}. At very high gas velocities a slight increase of the gas flow in the small gas bubbles is observed. At such a high gas velocity, turbulent eddies break-up large gas bubbles into small gas bubbles. This increases the gas hold-up of the small gas bubbles and correspondingly increases the small gas bubble flow. However, at the distributor the gas flow in the small gas bubbles can be assumed constant. In all the 10,000 video images captured during 10 s coalescence of small bubbles was hardly observed. To account for the generation of small gas bubbles from large gas bubbles, an additional constitutive equation is required, which is not developed in this work.

Model Results

The gas hold-up model was fitted to the experimental gas hold-up data for the air-water system and for the air-Isopar M system by a non-linear regression routine from MATLAB® 7.0 to evaluate the unknown model parameters λ and k. In Figure 12a, b, the fitting results are shown for the air-demineralised water and the air-Isopar M systems in the 29-cm column, respectively. The model fits the gas hold-up data in the homogeneous regime and the churn-turbulent regime. The experimentally observed local maximum and local minimum in the gas hold-up around the gas transition velocity are described by the model. In the model, the small bubble gas hold-up in the homogeneous regime increases till the regime transition point. In the churn-turbulent regime, the superficial liquid velocity increases in the riser by the increase in the large gas bubble hold-up. The Wallis drift flux theory predicts that the small gas bubble hold-up decreases with an increase in superficial liquid velocity and a constant superficial gas velocity. Therefore, the small gas bubble hold-up decreases sharply and a local maximum is observed at the regime transition point. The local minimum is caused by the steadily increasing large bubble gas hold-up and a small bubble gas hold-up that becomes approximately constant at a higher superficial gas velocity. The model fits well with the average superficial liquid velocity data for air-water system

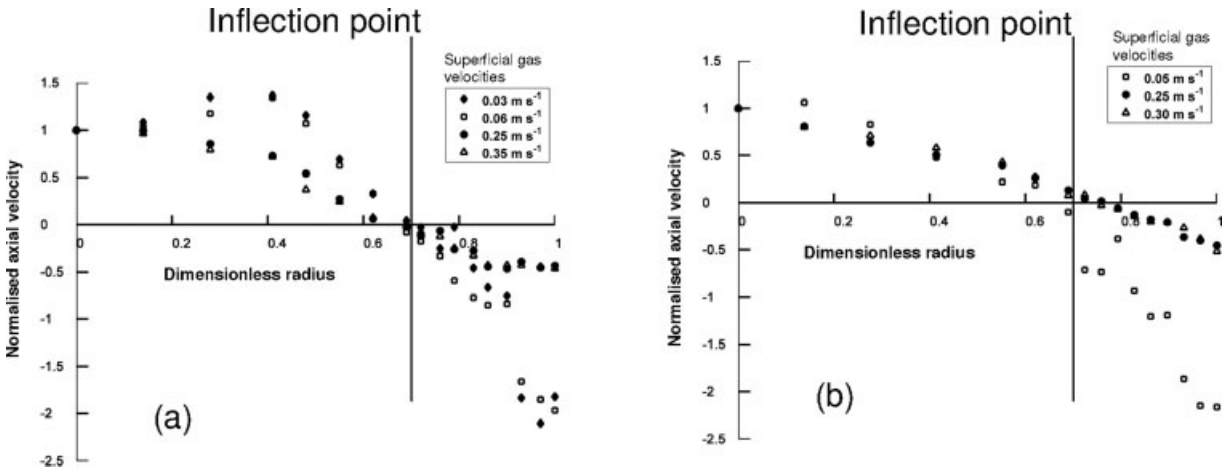

Figure 9. Radial profile of the axial superficial liquid velocities normalized with the centerline superficial liquid velocity.

The velocity profiles were measured in the homogeneous regime and the churn-turbulent regime at different superficial gas velocities mentioned in the legend. (a) Air-demineralised water system, (b) Air-Isopar M system. Inflection point for both systems was at $\delta = 0.7$.

in the homogeneous regime and the churn-turbulent regime. For the air-Isopar M system the fit is excellent in the churn-turbulent regime. The superficial liquid velocity data is overestimated in the homogeneous regime.

The values of λ and k with their confidence intervals are summarized in Table 2. The values of λ and k are higher for the air-Isopar M system. The lower value of λ for the air-water system indicates that the amount of small gas bubbles in the downer is lower than in the case of the air-Isopar M system. For the air-Isopar M system, the small gas bubbles are smaller than for the air-water system, (2–6 mm) and (3–6 mm) respectively, due to the lower surface tension of the air-Isopar M system. Therefore, the population of small gas bubbles in the riser is higher. The slip velocity is approximately equal to the one of the air-water system and thus, more small bubbles are dragged in the downer. The hold-up of small gas

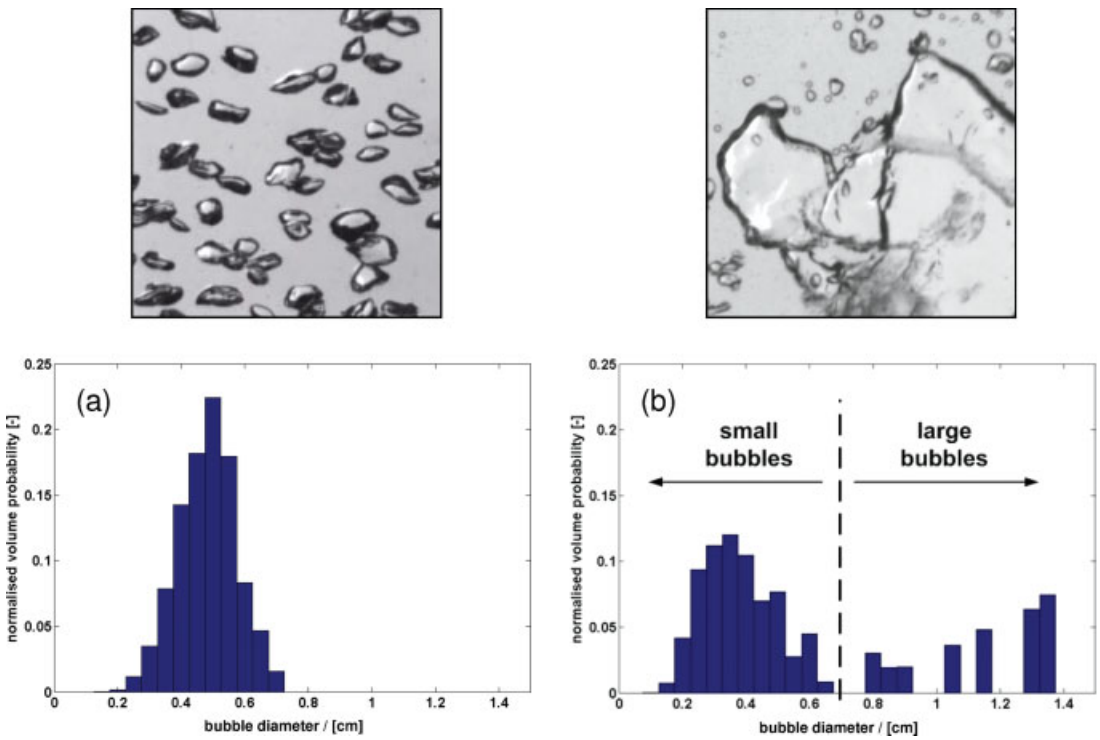

Figure 10. Bubble size distribution of the small gas bubbles in a pseudo-2D SBC reactor at different gas velocities.

(a) $u_g = 0.01$ m s^{-1}, (b) $u_g = 0.44$ m s^{-1}. Both video frames are 6 cm × 6 cm. [Color figure can be viewed in the online issue, which is available at www.interscience.wiley.com.]

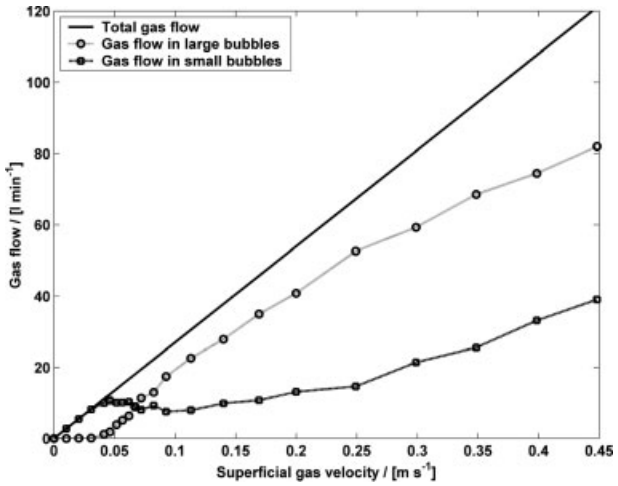

Figure 11. Distribution of the gas flow in the small and the large gas bubbles in a pseudo-2D SBC reactor.

bubbles in the downer increases and increases the value of λ for the air-Isopar M system. The higher viscosity of Isopar M increases the momentum dissipation by the bends, which is reflected by higher values of k when compared to water.

The value of λ was estimated for the air-water system by manually processing the videos obtained in the pseudo 2D SBC reactor. A value of 0.72 for λ was estimated from five frames at $u_g = 0.21$ m s^{-1}. The bubbles were manually counted from each frame to get the hold-up of the small gas bubbles in the downer and in the riser sections. The experimental value of λ from manual video processing is 16% higher than the value fitted with the model. Given the rather course manual determination of the experimental value for λ from video images, the agreement with the fitted value is quite satisfactory.

In Figure 13, the model results for demineralised water with carbon slurry concentrations are shown. The model describes the gas hold-up data accurately in the homogeneous and churn-turbulent regimes with the same values of λ and k as found in Figure 12 for the air-water system. The experimentally determined regime transition point decreases with an increase in slurry concentration. The gas hold-up data and the regime transition point can be found elsewhere[28]. The model can successfully determine the gas hold-up for slurry systems up to 3 vol % slurry concentration.

Model Validation

Literature gas hold-up data

Literature data was used to test the validity of the model. The gas hold-up data and the centerline liquid velocity data presented by Krishna et al.[34] and by Ruzicka et al.[35] were used for the air–water system. The data presented by Krishna et al.[36] were used for the air-Isopar M system and the centerline liquid velocities were converted to the average superficial liquid velocities for comparing them with the model predicted superficial liquid velocity values. The transition point as determined from the coherent standard deviation was not available in these cases, and thus the superficial gas velocity at the local maxima in the gas hold-up profile was used wherever possible. The values of λ and k from Table 2 were used to determine the gas hold-up and the average superficial liquid velocities of these different systems. An error of 3% is obtained between the literature gas hold-up data and the model as shown in Figure 14a for the air-water system. The model slightly over predicts the average superficial liquid velocities in the churn-turbulent regime. Figure 14b compares the air–water literature data from Ruzicka et al.[35] An error of 2% is obtained between the model and the data. Figure 15 gives the gas hold-up data of the air-Isopar M system from Krishna et al.[36] obtained in a column diameter of 0.29 m and liquid height of 1.74 m. The agreement obtained between the model predictions and the experimental data is good. These

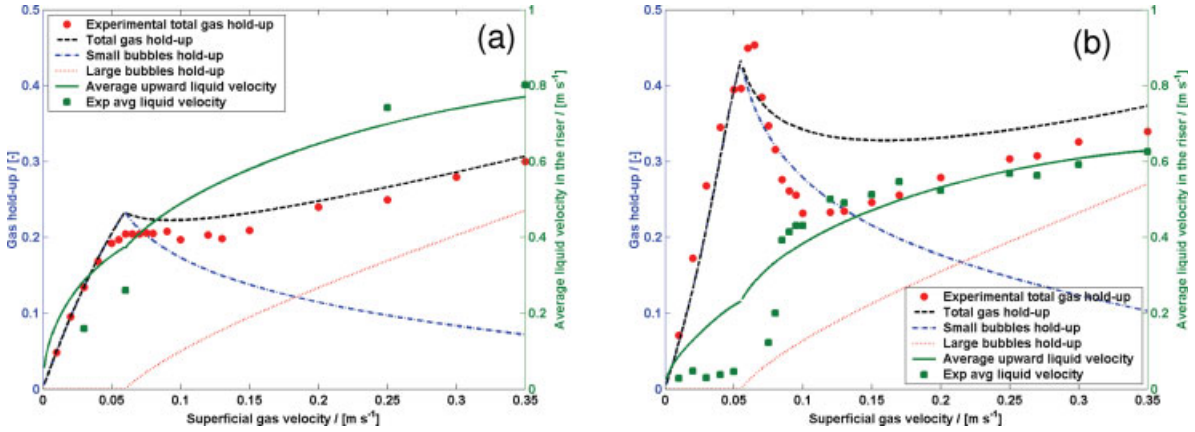

Figure 12. Gas hold-up model fitted to the experimental data obtained in: (a) air-demineralized water system, and (b) air-Isopar M system.

The small gas bubble hold-up, the large gas bubble hold-up, and the average superficial liquid velocity in the riser obtained from the model are also shown. [Color figure can be viewed in the online issue, which is available at www.interscience.wiley.com.]

Table 2. Values of the Unknown Model Parameters Obtained from Fitting the Gas Hold-up Model to the Experimental Data Obtained in the 29-cm Column for Air–Water System and Air-Isopar M System

Fitting Parameters	Air–Water	95% Confidence Interval (C.I.)	Air-Isopar M	95% Confidence Interval (C.I.)
λ	0.62	0.57–0.68	0.86	0.82–0.91
k	14.6	12.4–16.8	18.4	14.2–22.6

comparisons suggest that the model can be generally applied to a gas–liquid system with known physical properties with the values of k and λ presented here, although this has not been verified for more viscous systems.

There are numerous empirical gas hold-up models available in literature. Mostly these empirical correlations have more than five fitting parameters with limited physical significance.[3–7] An accurate prediction of the hydrodynamics of bubble column in the churn-turbulent regime by CFD models have not been presented yet in literature. Behkish et al.[37] proposed a novel correlation to predict gas hold-up in bubble columns. The authors propose that the model accounts for a number of criteria including the pressure and the temperature of the column. Their gas hold-up correlation was obtained from a least-squares fit of 3881 data points from various literature references. The gas hold-up predictions for air–water system from the Behkish et al.[37] model are compared with our experimental data in Figure 16a. The model shows good agreement in the churn-turbulent regime. In the homogeneous regime, however, it under-

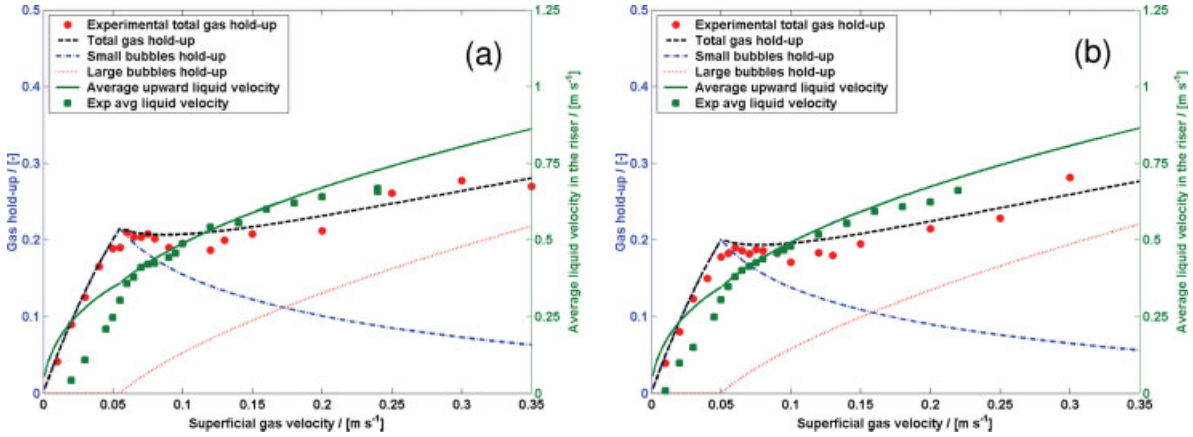

Figure 13. Model fitted to the gas hold-up and the average superficial liquid velocity data for the carbon slurries in the demineralized water.

(a) 0.7 vol %, (b) 1.4 vol %. [Color figure can be viewed in the online issue, which is available at www.interscience.wiley.com.]

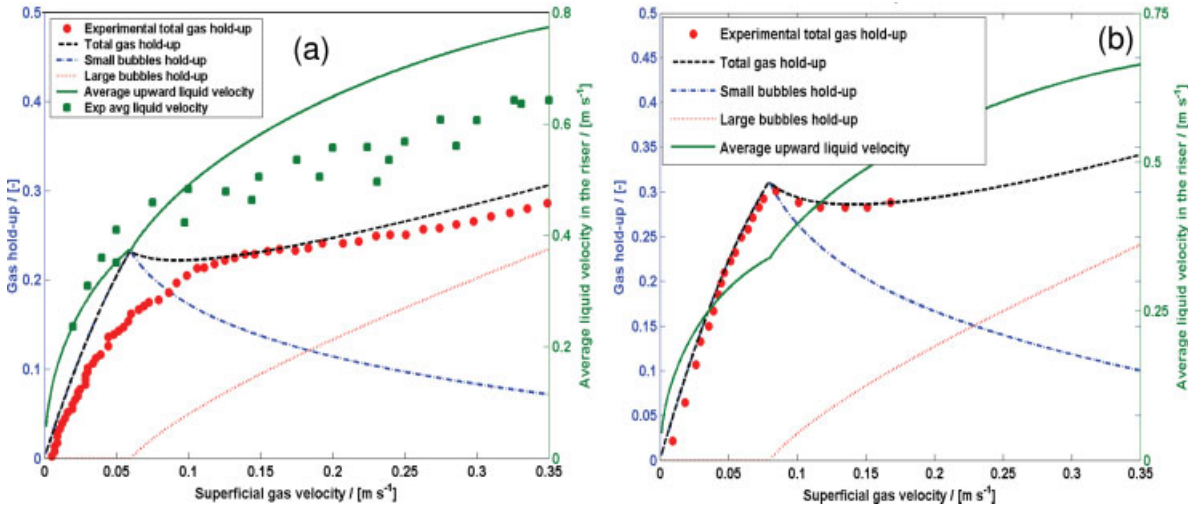

Figure 14. Validation of the gas hold-up model with two different literature data for the air-water systems.

(a) Data by Krishna et al.,[34] $D_c = 0.38$ m, $H = 1.7$ m, (b) data by Ruzicka et al.[35] $D_c = 0.29$ m, $H = 1.10$ m. [Color figure can be viewed in the online issue, which is available at www.interscience.wiley.com.]

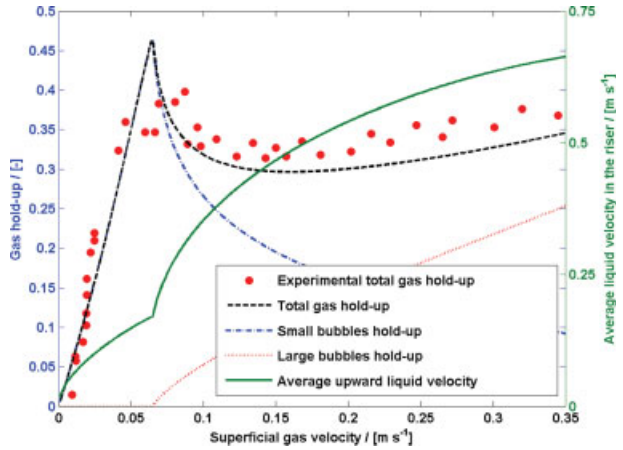

Figure 15. Validation of the gas hold-up model with literature experimental data for air-Isopar M system by Krishna et al.[36]

[Color figure can be viewed in the online issue, which is available at www.interscience.wiley.com.]

estimates the gas hold-up data. This model shows significant large gas bubble hold-up already in the homogeneous regime. This model does not predict the local maximum and minimum for the gas hold-up, which is a characteristic of a perforated plate sparger. In Figure 16b the Behkish et al. model underestimates the experimental data for the air-Isopar M system. The model is also insensitive to the initial liquid height.

Sensitivity of model for initial height of liquid and column diameter

The initial height of the liquid in the column, H, influences the gas hold-up significantly.[35] In Figure 17a, different initial liquid heights were used in the model for the same column diameter, D_c, and regime transition velocity, u_{trans}. The model predicts a decrease in the gas hold-up with increasing initial liquid height. A similar effect of initial liquid height was observed by Ruzicka et al.[35] The effect of the energy dissipation at the bends, k, becomes less significant compared to the wall friction as the liquid height increases. Therefore the liquid circulations become large which decreases the residence time of the gas in the column. This results in a lower gas hold-up as the liquid height increases.

Figure 17b shows the sensitivity of the model predictions for the column diameter. The initial liquid height was fixed to 1.7 m for this analysis. The figure shows that there is no significant influence of the column diameter on the gas hold-up. A similar effect of column diameter was observed by Yang and Fan.[38] The authors compared the effect of the diameter up to 5 m and showed that the column diameter has no effect on hydrodynamics if the initial height is fixed. Shah et al.[3] were one of the first to show the influence of column diameter on gas hold-up and found that for larger column diameters (higher than 15 cm), the gas hold-up remains constant.

Concluding Remarks

The model of the gas hold-up in a slurry bubble column presented in this paper predicts all the gas hold-up data used in this study with an error of less than 3%. The input parameters are the physical properties of the gas–liquid system (e.g. density, viscosity), column dimensions (diameter, height), and the flow regime transition point. In addition to the total gas hold-up, the model predicts the average liquid velocities, and the small and large gas bubble hold-ups in the riser and in the downer. The two parameters in the model, k and λ, were estimated by fitting it to the experimental data. Validation of the model with literature data demonstrates the applicability of the model for other liquid sys-

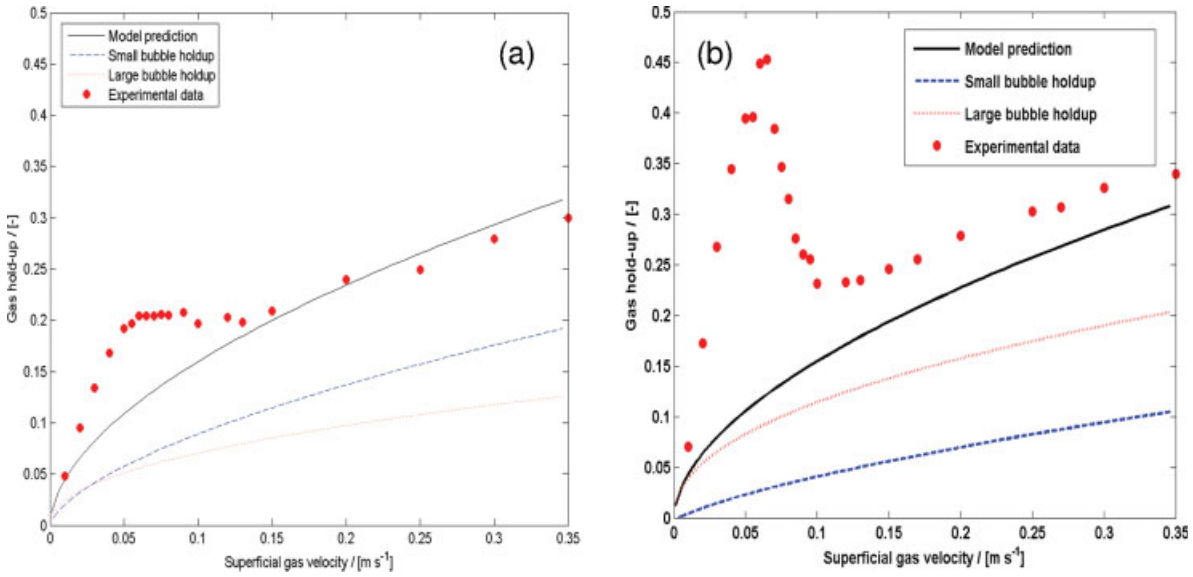

Figure 16. Gas hold-up prediction by Behkish et al.[37] compared to our experimental data.

[Color figure can be viewed in the online issue, which is available at www.interscience.wiley.com.]

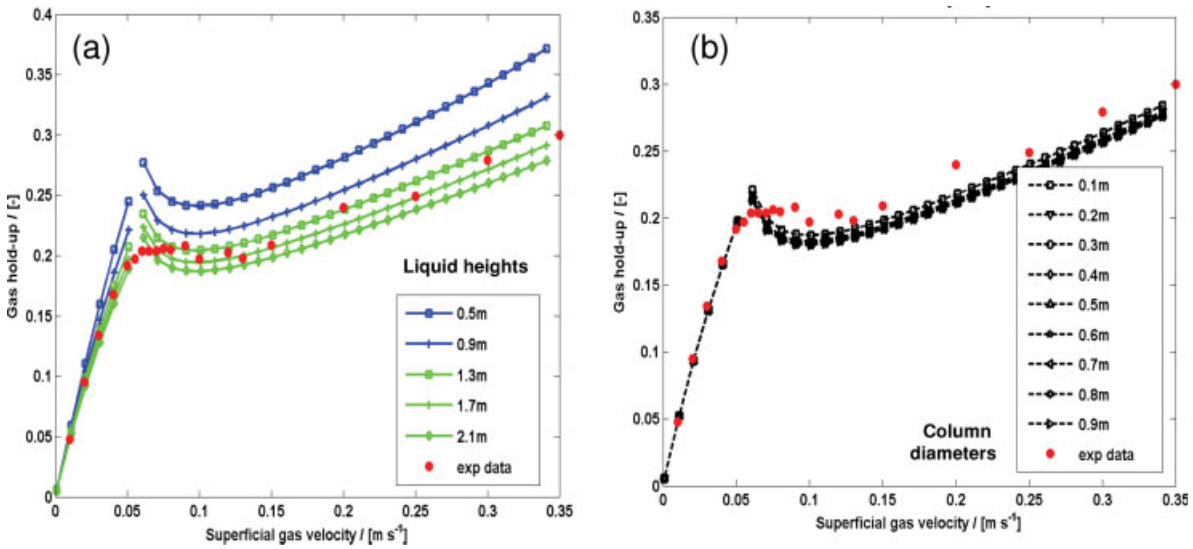

Figure 17. Sensitivity of the height and diameter in the model.

(a) Height sensitivity, (b) diameter sensitivity. [Color figure can be viewed in the online issue, which is available at www.interscience.wiley.com.]

tems. The model is validated for slurry concentrations up to 3 vol %. The gas hold-up in the SBC reactor is unaffected by the scale of the reactor at diameters larger than 15 cm.

Acknowledgments

The authors gratefully acknowledge the Dutch Technology Foundation STW (EPC. Project 5239), Akzo Nobel, DSM Research B.V., Shell Global Solutions, and Sasol Technology Netherlands for their financial support, and Engelhard B.V. and Norit for supplying the catalyst particles.

Notation

a = constant in Richardson and Zaki equation
A_{riser} [m^2] = cross-sectional area of the riser
A_{downer} [m^2] = cross-sectional area of the downer
A_{column} [m^2] = cross-sectional area of the SBC
d_{b} [m] = average bubble diameter
$d_{\text{b,large}}$ [m] = average large gas bubble diameter
$d_{\text{b,small}}$ [m] = average small gas bubble diameter
D_{c} [m] = diameter of the SBC
f = Fanning friction factor
f_{downer} = friction factor in the riser
f_{riser} = friction factor in the downer
g [m s^{-2}] = acceleration due to gravity
h_1, h_2 [m] = heights of the reference point
H [m] = initial liquid height
H_{s} [m] = height of the gas–liquid suspension
k = frictional losses due to bending of the flow
L_f [kg m s^{-1}] = momentum dissipation term
P_1, P_2 [Pa] = pressure at both the reference points
$\bar{p}$ [Pa] = average static pressure measured by pressure transducers
r = Dimensionless radius
Re_{l} = Reynolds number of the average liquid flow
Re_{∞} = Reynolds number of the small gas bubbles
$R_{\text{H,downer}}$ [m] = hydraulic diameter of the downer
$R_{\text{H,riser}}$ [m] = hydraulic diameter of the riser
$u_{\text{b},\infty}^{\text{large}}$ [m s^{-1}] = terminal rise velocity of the large gas bubbles
$u_{\text{b},\infty}^{\text{small}}$ [m s^{-1}] = terminal rise velocity of the small gas bubbles
u_{g} [m s^{-1}] = superficial gas velocity
$u_{\text{g,downer}}$ [m s^{-1}] = superficial gas velocity in the downer
$u_{\text{g,riser}}$ [m s^{-1}] = superficial gas velocity in the riser
$u_{\text{l,downer}}$ [m s^{-1}] = average superficial downward liquid velocity in the downer
$u_{\text{l,riser}}$ [m s^{-1}] = average superficial upward liquid velocity in the riser
$u_{\text{l,c}}$ [m s^{-1}] = centerline liquid velocity in the riser
u_{l} [m s^{-1}] = interstitial liquid velocity
U_{slip} [m s^{-1}] = slip velocity between small gas bubbles and liquid in the riser
u_{trans} [m s^{-1}] = regime transition gas velocity
V_1, V_2, V_l [m s^{-1}] = interstitial liquid velocity
δ = dimensionless diameter of the riser in the column
$\varepsilon_{\text{g,downer}}$ = gas hold-up in the downer
$\varepsilon_{\text{g,riser}}$ = gas hold-up in the riser
ε_{g} = overall gas hold-up
$\varepsilon_{\text{g,small}}$ [$\text{m}^3_{\text{gas}}/\text{m}^3_{\text{riser}}$] = Hold-up of small gas bubbles in the liquid phase in the riser
$\varepsilon_{\text{g,large}}$ = Hold-up of large gas bubbles in the riser
λ = ratio of the small gas bubble hold-up in the riser to that in the downer
μ_l [Pa s] = viscosity of the liquid phase
ρ_{g} [kg m^{-3}] = density of the gas phase
ρ_l [kg m^{-3}] = density of the liquid phase
$\Delta\rho$ [kg m^{-3}] = density difference between the liquid phase and gas phase
σ_1 [N m^{-1}] = surface tension of the liquid phase

Literature Cited

1. Krishna R, Ellenberger J, Hennephof DE. Analogous description of the hydrodynamics of gas-solid fluidized beds and bubble columns. *Chem Eng J*. 1993;53:89–101.
2. Krishna R, Ellenberger J. Gas Holdup in bubble column reactors operating in the churn-turbulent flow regime. *AIChE J*. 1996;42:2627–2634.
3. Shah YT, Kelkar BG, Godbole SP, Deckwer W-D. Design parameters estimations for bubble column reactors. *AIChE J*. 1982;28:353–379.

4. Deckwer W-D. Bubble Column Reactors. Chichester: Wiley, 1992.
5. Joshi JB, Parasu Veera U, Prasad ChV, Phanikumar DV, Deshphande NS, Thakre SS, Thorat BN. Gas hold-up structure in bubble column reactors. *PINSA*. 1998;64A:441–567.
6. Joshi JB, Vitankar VS, Kulkarni AA, Dhotre MT, Ekambara K. Coherent flow structures in bubble column reactors. *Chem Eng Sci*. 2002;57:3157–3183.
7. Wild G, Poncin S, Li HZ, Olmos E. Some Aspects of the hydrodynamics of bubble columns. *Int J Chem React Eng*. 2003;1:R7
8. Gupta P, Ong B, Al Dahhan MH, Dudukovic MP, Toseland BA. Hydrodynamics of churn turbulent bubble columns: gas-liquid recirculation and mechanistic modeling. *Catal Today*. 2001;64:253–269.
9. Joshi JB. Computational flow modelling and design of bubble column reactors. *Chem Eng Sci*. 2001;56:5893–5933.
10. Pan Y, Dudukovic MP, and Chang M. Dynamic simulation of bubbly flow in bubble columns. *Chem Eng Sci*. 1999;54:2481–2489.
11. Dudukovic MP. Opaque multiphase flows: experiments and modeling. *Exp Therm Fluid Sci*. 2002;26:747–761.
12. Rietema K, Ottentgraf PP. Laminar liquid circulation and bubble street formation in a gas-liquid system. *Trans Inst Chem Eng*. 1970;48:T54–T62.
13. Rice RG, Geary NW. Prediction of liquid circulation in viscous bubble columns. *AIChE J*. 1990;36:1339–1348.
14. Kawase Y, Umeno S, Kumagai T. The Prediction of gas hold-up in bubble column reactors: newtonian and non-newtonian fluids. *Chem Eng J*. 1992;50:1–7.
15. Burns LF, Rice RG. Circulation in bubble columns. *AIChE J*. 1997;43:1390–1402.
16. Lin T-J, Reese J, Hong T, Fan L-S. Quantitative analysis and computation of two-dimensional bubble colums. *AIChE Journal*. 1996;42:301–318.
17. Ulbrecht JJ, Kawase Y, Auyeung KF. More on mixing of viscous liquids in bubble columns. *Chem Eng Commun*. 1985;35:175–191.
18. Bird RB, Stewart WE, Lightfoot EN. Transport phenomena. Singapore: Wiley, 1960.
19. Krishna R, Wilkinson PM, Dierendonck LLv. A model for gas holdup in bubble columns incorporating the influence of gas density on flow regime transitions. *Chem Eng Sci*. 1991;46:2491–2496.
20. Krishna R, Urseanu MI, Van Baten JM, Ellenberger J. Rise velocity of a single circular cap bubbles in two dimensional beds of powders and liquids. *Chem Eng Proc*. 1999;39:433–440.
21. May WG. Fluidized bed reactor studies. *Chem Eng Prog*. 1959;55:49–56.
22. Van Deemter JJ. Mixing and contacting in gas-solid fluidized beds. *Chem Eng Sci*. 1961;13:143–154.
23. Wesselingh JA. The velocity of particles, drops, and bubbles. *Chem Eng Proc*. 1987;21:9–14.
24. Davies RM, Taylor G. The mechanics of large bubbles rising through extended liquids and through liquids in tubes. *Proc R Soc London Ser A*. 1950;200:375–390.
25. Ruzicka MC, Zahradnik J, Drahos J, Thomas NH. Homogeneous-heterogeneous regime transition in bubble columns. *Chem Eng Sci*. 2001;56:4609–4626.
26. Vial C, Camarasa E, Poncin S, Wild G, Midoux N, Bouillard J. Study of hydrodynamic behaviour in bubble columns and external loop airlift reactors through analysis of pressure fluctuations. *Chem Eng Sci*. 2000;55:2957–2973.
27. Zahradnik J, Fialova M, Ruzicka MC, Drahos J, Kastanek F, Thomas NH. Duality of gas-liquid flow regimes in bubble column reactors. *Chem Eng Sci*. 1997;52:3811–3826.
28. Ruthiya KC, Chilekar VP, Warnier M, van der Schaaf J, van Ommen JR, Kuster BFM, Schouten JC. Detecting regime transitions in slurry bubble columns using pressure time series. *AIChE J*. 2005;51:1951–1965.
29. Richardson JF, Zaki WN. Sedimentation and Fluidisation: Part 1. *Trans Inst Chem Eng*. 1954;32:35
30. Wallis GB. One Dimensional Two-Phase Flow. New York: McGraw-Hill, 1969.
31. Chilekar VP, Warnier MJF, van der Schaaf J, van Ommen JR, Kuster BFM, Schouten JC. Bubble size estimation in slurry bubble columns from pressure fluctuations. *AIChE J*. 2005;51:1924–1937.
32. Ueyama K, Miyauchi T. Properties of recirculating turbulent two phase flow in gas bubble columns. *AIChE J*. 1979;25:258–265.
33. Urseanu MI. Scaling up bubble column reactors, PhD Thesis. University of Amsterdam, The Netherlands, 2000.
34. Krishna R, Urseanu MI, Van Baten JM, Ellenberger J. Rise velocity of a swarm of large gas bubbles in liquids. *Chem Eng Sci*. 1998;54:171–183.
35. Ruzicka MC, Drahos J, Fialova M, Thomas NH. Effect of bubble column dimensions on flow regime transition. *Chem Eng Sci*. 2001;56:6117–6124.
36. Krishna R, Deswart JWA, Ellenberger J, Martina GB, Maretto C. Gas Holdup in Slurry Bubble-Columns—effect of column diameter and slurry concentrations. *AIChE J*. 1997;43:311–316.
37. Behkish A, Lemoine R, Oukaci R, Morsi BI. Novel correlations for gas holdup in large-scale slurry bubble column reactors operating under elevated pressures and temperatures. *Chem Eng J*. 2006;115:157–171.
38. Yang GQ, Fan LS. Axial liquid mixing in high-pressure bubble columns. *AIChE J*. 2003;49:1995–2008.

Appendix: Momentum Balance over the Circulation Loop

A momentum balance is set-up for the two phase flow along the height of the riser and the downer to obtain the liquid circulation velocity and this balance is presented as in Eq. 1. The liquid circulation path in the riser and in the downer used for the momentum balance is shown in Figure 4. The complete balance is achieved by integrating Eq. 1 over the circulation path in the riser and in the downer. Applying Eq. 1 to the circulation path in the riser gives:

$$(1-\varepsilon_{g,riser})\rho_l\frac{\partial u_{l,riser}}{\partial t}+\varepsilon_{g,riser}\rho_g\frac{\partial u_{g,riser}}{\partial t}= -(1-\varepsilon_{g,riser})\rho_l u_{l,riser}\left(\frac{\partial u_{l,riser}}{\partial h}\right)-\varepsilon_{g,riser}\rho_g u_{g,riser}\left(\frac{\partial u_{g,riser}}{\partial h}\right) -\frac{\partial P}{\partial h}+((1-\varepsilon_{g,riser})\rho_l+\varepsilon_{g,riser}\rho_g)g+L_{f,riser} \quad (A1)$$

Applying Eq. 1 to the second half of the circulation loop in the downer section gives:

$$(1-\varepsilon_{g,downer})\rho_l\frac{\partial u_{l,downer}}{\partial t}+\varepsilon_{g,downer}\rho_g\frac{\partial u_{g,downer}}{\partial t}= -(1-\varepsilon_{g,downer})\rho_l u_{l,downer}\left(\frac{\partial u_{l,downer}}{\partial h}\right) -\varepsilon_{g,downer}\rho_g u_{g,downer}\left(\frac{\partial u_{g,downer}}{\partial h}\right)-\frac{\partial P}{\partial h}+((1-\varepsilon_{g,downer})\rho_l +\varepsilon_{g,downer}\rho_g)g+L_{f,downer} \quad (A2)$$

where $L_{f,downer}, L_{f,riser}$ are the wall frictional losses in the downer and in the riser, respectively. Although there is only a virtual wall between the downer and the riser, the superficial liquid velocity equals zero as it would for a solid wall (Figure 2). Thus, the no-slip condition also holds for the virtual wall. Thus in the riser, the wall frictional losses are used to approximate the pressure losses. At steady state, integrating over the riser from the position 2 to 1 as shown in the Figure 4 gives:

$$0=-\int_2^1\left((1-\varepsilon_{g,riser})\rho_l\left(\frac{\partial}{\partial h}\frac{u_{l,riser}^2}{2}\right)\right) -\int_2^1\left(\varepsilon_{g,riser}\rho_g\left(\frac{\partial}{\partial h}\frac{u_{l,riser}^2}{2}\right)\right)\cdots-\int_2^1\frac{\partial P}{\partial h}$$

$$+\int_2^1((1-\varepsilon_{g,riser})\rho_l+\varepsilon_{g,riser}\rho_g)g+\int_2^1 L_{f,riser} \quad (A3)$$

Simplifying Eq. A3 further gives:

$$-L_{f,riser}(h_1-h_2)+(P_1-P_2)=(1-\varepsilon_{g,riser})\rho_l g(h_1-h_2) \quad (A4)$$

since $\rho_g<\rho_l, U_{l,riser,2}=U_{l,riser,1}$ and $U_{g,riser,2}=U_{g,riser,1}$. Similarly, Integrating Eq. A2 in the downer between the points 1 and 2 and further simplifying gives:

$$-L_{f,downer}(h_1-h_2)+(P_1-P_2)=(1-\varepsilon_{g,downer})\rho_l g(h_1-h_2) \quad (A5)$$

Overall balance over the complete circulation loop is achieved by subtracting Eq. 29 from Eq. 30 to get the following:

$$L_{f,downer}(h_1-h_2)+L_{f,riser}(h_1-h_2) = (\varepsilon_{g,riser}-\varepsilon_{g,downer})\rho_l g(h_1-h_2) \quad (A6)$$

The frictional loss terms are given as:[18]

$$L_f=\frac{P_w\tau_w}{A}=\frac{\pi D_j\tau_w}{\frac{\pi}{4}D_j^2} \quad (A7)$$

where P_W is the wetted perimeter, τ_W is the shear stress at wall, A is the cross sectional area of the riser or of the downer section, and subscript j is either the riser or the downer. The wall shear stress is given by:[18]

$$\tau_w=\frac{\frac{1}{2}\rho_l f_j u_{l,j}^2}{(1-\varepsilon_{g,j})} \quad (A8)$$

Therefore Eq. A7 takes the form:

$$L_f=\frac{\frac{1}{2}\rho_l f_j u_{l,j}^2}{R_{H,j}(1-\varepsilon_{g,j})} \quad (A9)$$

Furthermore, there are singular pressure losses at the two turning points. Both the losses, one at the top of the downer at the position 1 and one at the bottom of the downer at the position 2, are given by:

$$\Delta p_1=\frac{\frac{1}{2}\rho_l k_1 u_{l,downer}^2}{1-\varepsilon_{g,downer}}$$
$$\Delta p_2=\frac{\frac{1}{2}\rho_l k_2 u_{l,downer}^2}{(1-\varepsilon_{g,downer})} \quad (A10)$$

where $k_1=k_2=k$ are the frictional losses due to the bending of the liquid at the top and the bottom of the column. These losses are added to the left hand side of the Eq. A6

$$L_{f,downer}(h_1-h_2)+\Delta\rho_l+L_{f,riser}(h_1-h_2)+\Delta p_2 = (\varepsilon_{g,riser}-\varepsilon_{g,downer})\rho_l g(h_1-h_2) \quad (A6)$$

From Eqs. A9–A11 the final form of the overall momentum balance becomes:

$$(\varepsilon_{g,riser}-\varepsilon_{g,downer})g=\left(\frac{f_{downer}}{R_{H,downer}}+\frac{2k}{H_s}\right)\left(\frac{\frac{1}{2}u_{l,downer}^2}{1-\varepsilon_{g,downer}}\right)+\left(\frac{f_{riser}}{R_{H,riser}}\right)\left(\frac{\frac{1}{2}u_{l,riser}^2}{1-\varepsilon_{g,riser}}\right) \quad (A12)$$

Equation A12 gives the momentum balance over the complete circulation loop in the riser and the downer.

Manuscript received Sept. 14, 2006, and revision received Mar. 20, 2007.